Investigation of the structural, optical and magnetic properties of nickel ferrite nanoparticles synthesized through modified sol–gel method

S. Akbar Hoseini[1] · Saeid Khademolhoseini[2]

Abstract Nickel ferrite nanoparticles were successfully synthesized by through modify sol–gel method with the aid of nickel (II) nitrate, iron (III) nitrate, and lactose without adding external surfactant. Moreover, lactose plays role as capping agent, reducing agent, and natural template in the synthesis of $NiFe_2O_4$ nanoparticles. The as-synthesized $NiFe_2O_4$ nanoparticles were characterized by means of several techniques such as X-ray diffraction, scanning electron microscopy, energy dispersive X-ray microanalysis and UV–Vis diffuse reflectance spectroscopy. The magnetic properties of as-prepared $NiFe_2O_4$ nanoparticles were also investigated with vibrating sample magnetometer. To evaluate the photocatalyst properties of nanocrystalline $NiFe_2O_4$, the photocatalytic degradation of methyl orange under ultraviolet light irradiation was carried out.

1 Introduction

Nanoscale materials have attracted significant scientific and industrial interest during the last decade [1–6]. These materials are novel compounds of theoretical interest currently, but have huge potential to develop as important classes of materials for the electronics and Photonics industries in the current century [7–11]. The spinel ferrites of general formula MFe_2O_4, where M = Mn, Co, Ni, Zn, attract considerable interest as soft magnetic materials for potential applications in magnetic field sensing, ferrofluids, magnetic drug delivery, magnetic information storage, and high frequency devices. The advantage of these materials is in high magnetostriction and high rate of change of strain with magnetic field [12]. In recent years the evolution of physical properties of materials upon transition from macroscopic bulk state to the nanocrystalline one have been intensively investigated. This transition is accompanied by substantial changes of electronic structure: the continuous density of states is replaced by set of discrete levels the exact position of which is determined by a particle size [13]. With decreasing a particle size the fraction of surface atoms with smaller coordination number, broken chemical bonds, and disrupted local symmetry, also increases. Owing to these reasons not only the properties of surface atoms differ substantially from those of atoms in a particle core, but also the character of interactions between these groups of atoms can have additional peculiarities. All these factors result in appearance of principally new physical properties of nanocrystalline state as compared to the bulk one. For the spinel ferrites in ultradisperse and nanocrystalline states the cation distribution, and degree of inversion can differ from the corresponding bulk values which results in variation of magnetic and magnetoelastic properties. Strong dependence on preparation method [14, 15], thermal treatment conditions [12], particle size [16], and morphology [17, 18] was observed. Various methods have been developed for preparation of ultradisperse and nanocrystalline powders of spinel ferrites, namely the sol–gel [19, 20], hydrothermal synthesis [14, 15], organic complexes, combustion processes with various precursors [18, 21–25]. These applications mainly depend upon microstructure and surface properties of the fine powders which depend upon the method of preparation. Modify sol–gel method has the advantages of using inexpensive

✉ Saeid Khademolhoseini
saeid.khademolhoseini@gmail.com

1 Young Researchers and Elite Club, Science and Research Branch, Islamic Azad University, Tehran, Iran

2 Young Researchers and Elite Club, South Tehran Branch, Islamic Azad University, Tehran, Iran

precursors, low external energy consumption and resulting nano sized, homogenous highly reactive powder. In this report, for the first time, we had presented the green approach for preparation of $NiFe_2O_4$ nanoparticles by modify sol–gel method in the presence of lactose without adding external. This approach is simple and friendly to the environment. Moreover, the photocatalytic activities of $NiFe_2O_4$ catalysts were studied for the mineralization of methyl orange under ultraviolet light [26, 27].

2 Experimental

2.1 Characterization

X-ray diffraction (XRD) patterns were recorded by a Philips-X'PertPro, X-ray diffractometer using Ni-filtered Cu Kα radiation at scan range of $10 < 2\theta < 80$. Scanning electron microscopy (SEM) images were obtained on LEO-1455VP equipped with an energy dispersive X-ray spectroscopy. The energy dispersive spectrometry (EDS) analysis was studied by XL30, Philips microscope. The magnetic measurement of samples were carried out in a vibrating sample magnetometer (VSM) (Meghnatis Daghigh Kavir Co.; Kashan Kavir; Iran) at room temperature in an applied magnetic field sweeping between ±10,000 Oe. Spectroscopy analysis (UV–Vis) was carried out using shimadzu UV–Vis scanning UV–Vis diffuse reflectance spectrometer.

2.2 Synthesis of $NiFe_2O_4$ nanoparticles

In this work, 1 and 2 mmol of $Ni(NO_3)_2 \cdot 6H_2O$ and $Fe(NO_3)_3 \cdot 9H_2O$ were dissolved in 30 ml distilled water under stirring at room temperature. Then, a solution containing 1 mmol of lactose was added drop wise into the above mention solution and was kept stirring to form a gel at 90 °C. Finally, the obtained product was placed in a conventional furnace in air atmosphere for 2 h and calcine at 800 °C. After thermal treatment, the system was allowed to cool to room temperature naturally, and the obtained precipitate was collected.

2.3 Photocatalysis experiments

The methyl orange (MO) photodegradation was examined as a model reaction to evaluate the photocatalytic activities of the $NiFe_2O_4$ nanoparticles. The photocatalytic experiments were performed under an irradiation ultraviolet light. The photocatalytic activity of nanocrystalline $NiFe_2O_4$ obtained was studied by the degradation of methyl orange solution as a target pollutant. The photocatalytic degradation was performed with 50 ml solution of methyl orange

(0.0005 g) containing 0.1 g of $NiFe_2O_4$. This mixture was aerated for 30 min to reach adsorption equilibrium. Later, the mixture was placed inside the photoreactor in which the vessel was 15 cm away from the ultraviolet source of 400 W mercury lamps. The photocatalytic test was performed at room temperature. Aliquots of the mixture were taken at definite interval of times during the irradiation, and after centrifugation they were analyzed by a UV–vis spectrometer. The methyl orange (MO) degradation percentage was calculated as:

$$\text{Degradation rate } (\%) = 100(A_0 - A_t) / A_0 \qquad (1)$$

where A_t and A_0 are the obtained absorbance value of the methyl orange solution at t and 0 min by a UV–vis spectrometer, respectively.

3 Results and discussion

Crystalline structure and phase purity of as-prepared product has been determined using XRD. The XRD pattern of the $NiFe_2O_4$ in presence of is shown in Fig. 1. The XRD pattern of the as-synthesized $NiFe_2O_4$ nanoparticles indicates the formation of cubic phase of $NiFe_2O_4$ (JCPDS No. 03-0875) with the calculated cell parameter of a = b = c 8.3400 Å. According to XRD data, the crystallite diameter (D_c) of $NiFe_2O_4$ nanoparticles are calculated to be 35 nm using the Scherer Eq. (2):

$$D_c = K\lambda / \beta\cos\theta \qquad (2)$$

where β is the breadth of the observed diffraction line at its half intensity maximum, K is the so-called shape factor, which usually takes a value of about 0.9, and λ is the wavelength of X-ray source used in XRD. The morphology of the nanoparticles was investigated using SEM which demonstrates uniform nanoparticles with spherical shape homogenously distributed all over the sample, as it could be clearly observed in Fig. 2. The $NiFe_2O_4$ nanoparticles with particle size of about 40–50 nm were observed. The EDS analysis measurement was used to investigate the chemical composition and purity of $NiFe_2O_4$ nanoparticles. According to the Fig. 3, the product consists of Ni, Fe, and O elements. Furthermore, neither N nor C signals were detected in the EDS spectrum, which means the product is pure and free of any surfactant or impurity. The hysteresis loop of $NiFe_2O_4$ nanoparticles was studied to examine their magnetic properties (Fig. 4). At 300 K the remanent magnetization (Mr) is 10 emu/g, the coercive field (Hc) is 100 Oe and the magnetization at saturation (Ms) is estimated to be only 30 emu/g (the saturation magnetization Ms was determined from the extrapolation of curve of H/M vs. H). The diffused reflectance spectrum of the as-prepared $NiFe_2O_4$ nanoparticles is shown in Fig. 5. The
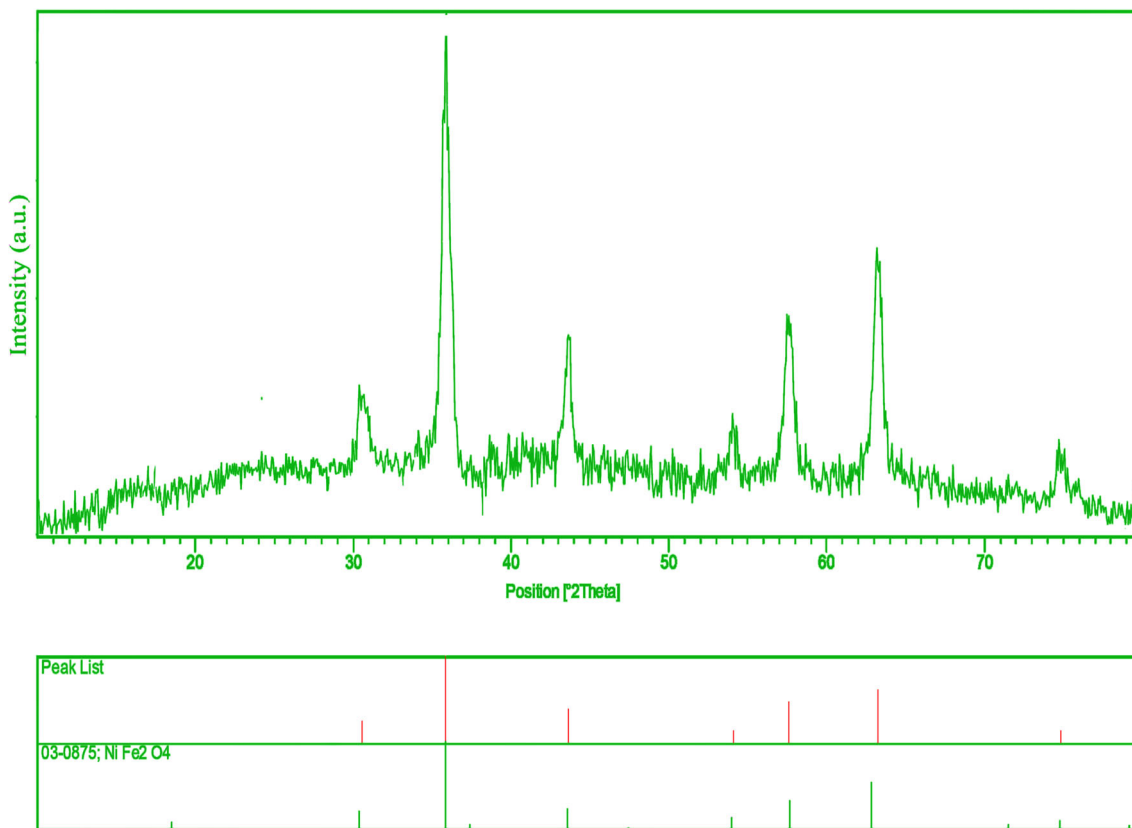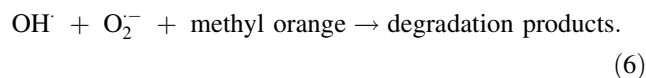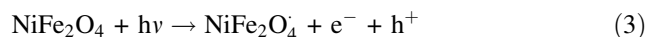
Fig. 1 XRD pattern of NiFe$_2$O$_4$ nanoparticles calcined at 800 °C

diffused reflectance spectrum of the as-prepared NiFe$_2$O$_4$ nanoparticles is shown in Fig. 5. The fundamental absorption edge in most semiconductors follows the exponential law. Using the absorption data the band gap was estimated by Tauc's relationship:

$$\alpha = \alpha 0 (h\nu - Eg)n/h\nu$$

where α is absorption coefficient, hν is the photon energy, $\alpha 0$ and h are the constants, E$_g$ is the optical band gap of the material, and n depends on the type of electronic transition and can be any value between 0.5 and 3. The energy gap of the NiFe$_2$O$_4$ nanoparticles is determined by extrapolating the linear portion of the plots of $(\alpha h\nu)^2$ against hν to the energy axis, as shown in Fig. 5. The E$_g$ value is calculated as 2.85 eV for the NiFe$_2$O$_4$ nanoparticles. Photodegradation of methyl orange (MO) as water contaminant under UV light illumination was employed to evaluate the properties of the as-synthesized NiFe$_2$O$_4$ nanoparticles. Figure 6 exhibits the obtained result. No methyl orange was practically broken down after 90 min without employing UV light illumination or as-prepared nanoparticles NiFe$_2$O$_4$. This observation illustrated that the contribution of self-degradation was insignificant. The proposed mechanism of the photocatalytic degradation of the methyl orange can be assumed as:

$$NiFe_2O_4 + h\nu \rightarrow NiFe_2O_4^{\cdot} + e^- + h^+ \tag{3}$$

$$h^+ + H_2O \rightarrow OH^{\cdot} \tag{4}$$

$$e^- + O_2 \rightarrow O_2^{\cdot -} \tag{5}$$

$$OH^{\cdot} + O_2^{\cdot -} + \text{methyl orange} \rightarrow \text{degradation products.} \tag{6}$$

Utilizing photocatalytic calculations by Eq. (1), the methyl orange degradation was about 52 % after 90 min illumination of UV light. This obtained result demonstrates that as-prepared NiFe$_2$O$_4$ nanoparticles have high potential to be applied as favorable and appropriate material for photocatalytic applications under illumination of UV light. The heterogeneous photocatalytic processes have diffusion, adsorption and reaction steps. It has been shown that the desirable distribution of the pore has effective and important impact on the diffusion of the reactants and products, and therefore effects on the photocatalytic activity. It seems that the enhanced photocatalytic activity of the as-obtained nanoparticles NiFe$_2$O$_4$ can be owing to desirable and
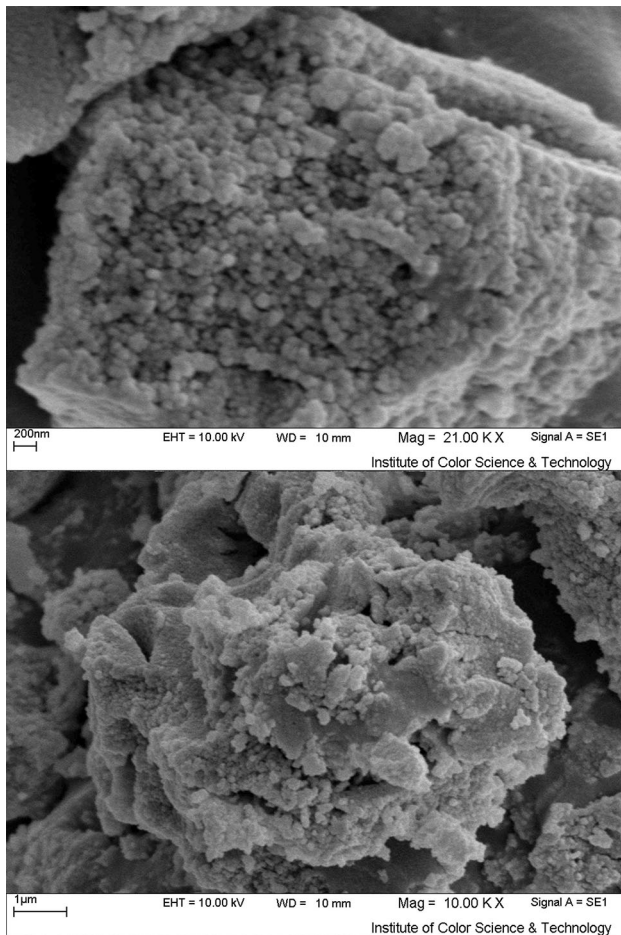
Fig. 2 SEM image of NiFe$_2$O$_4$ nanoparticles calcined at 800 °C

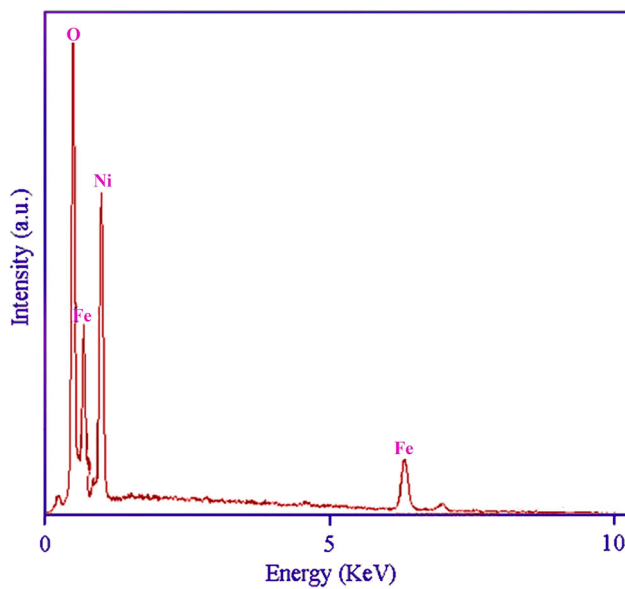

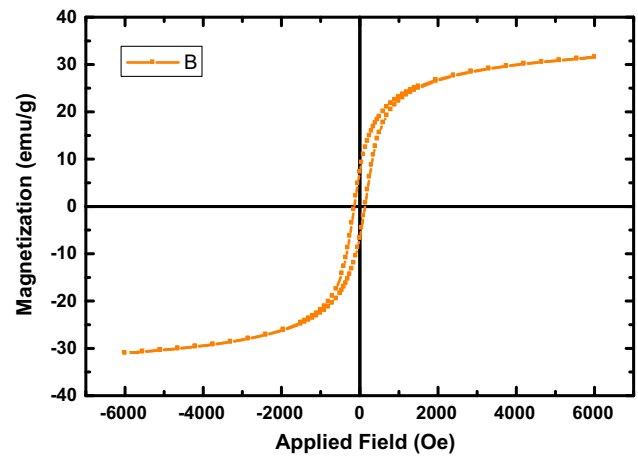Fig. 3 EDS pattern of NiFe$_2$O$_4$ nanoparticles calcined at 800 °C

Fig. 4 VSM curves of NiFe$_2$O$_4$ nanoparticles calcined at 800 °C
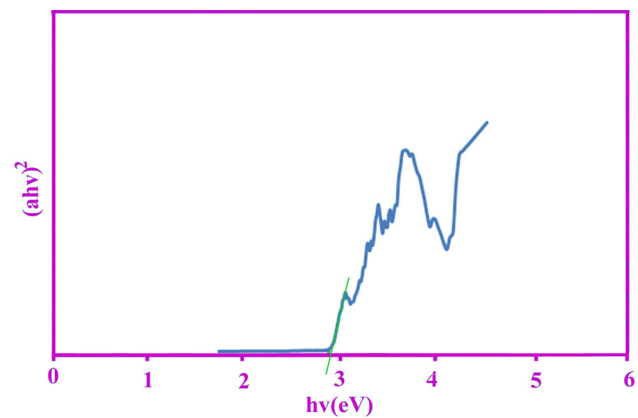

Fig. 5 Tauc plot pattern of NiFe$_2$O$_4$ nanoparticles calcined at 800 °C
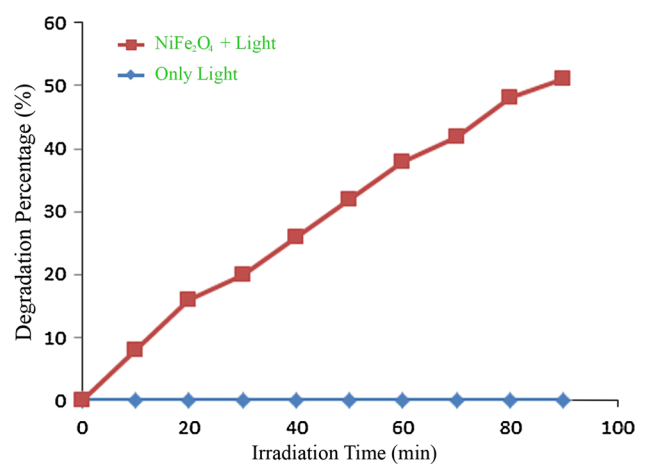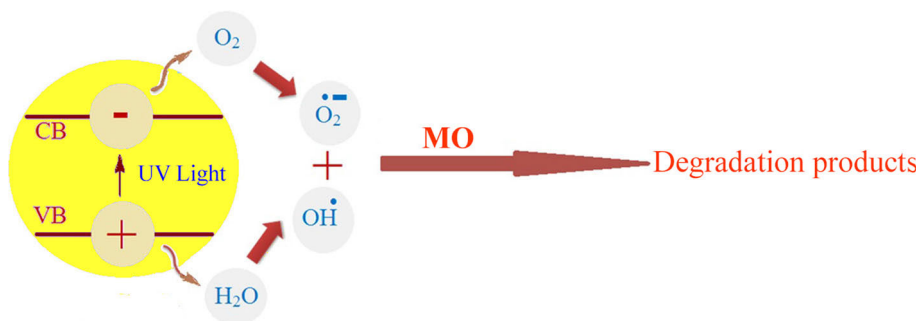

Fig. 6 Photocatalytic methyl orange degradation of NiFe$_2$O$_4$ nanoparticles under ultraviolet light

Scheme 1 Reaction mechanism of methyl orange photodegradation over $NiFe_2O_4$ nanoparticles under UV light irradiation

appropriate distribution of the pore, high hydroxyl amount and high separation rate of charge carriers (Scheme 1).

4 Conclusions

$NiFe_2O_4$ nanoparticles have been successfully synthesized through modify sol–gel method. Moreover, this method is free from any surfactant and organic solvents. High purity of the as-prepared nanocrystalline sample was proved by XRD, and EDS analyses. VSM analyzes indicates a paramagnetic behavior for the synthesized nanoparticles. When as-prepared nanocrystalline $NiFe_2O_4$ was utilized as photocatalyst, the percentage of methyl orange degradation was about 52 % after 90 min irradiation of UV light.

References

1. A. Abedini, S. Khademolhoseini, J. Mater. Sci. Mater. Electron. **27**, 330 (2016)
2. P. Bakhshaei, A. Ataie, H. Abdizadeh, J. NanoStruct. **3**, 403 (2013)
3. M. Rahimi-Nasarabadi, J. NanoStruct. **4**, 211 (2014)
4. M. Najafi, H. Haratizadeh, M. Ghezellou, J. NanoStruct. **5**, 129 (2015)
5. M. Ahmadzadeh, M. Almasi-Kashia, A. Ramazani, J. NanoStruct. **5**, 97 (2015)
6. F.S. Ghoreishi, V. Ahmadi, M. Samadpourc, J. NanoStruct. **3**, 453 (2013)
7. M. Rahimi-Nasrabadi, S.M. Pourmortazavi, M.R. Ganjali, Mater. Manuf. Process. **30**, 34 (2015)
8. M. Rahimi-Nasrabadi, S.M. Pourmortazavi, M.R. Ganjali, S.S. Hajimirsadeghi, M.M. Zahedi, J. Mol. Struct. **10**, 31 (2013)
9. S. Moshtaghia, D. Ghanbarib, M. Salavati-Niasari, J. NanoStruct. **5**, 169 (2015)
10. A. Rahdar, M. Aliahmad, Y. Azizi, J. NanoStruct. **5**, 145 (2015)
11. J. Safaei-Ghomi, S. Zahedi, M. Javid, M.A. Ghasemzadeh, J. NanoStruct. **5**, 153 (2015)
12. I.C. Nlebedim, N. Ranvah, P.I. Williams, Y. Melikhov, J.E. Snyder, A.J. Moses, D.C. Jiles, J. Magn. Magn. Mater. **322**, 1929 (2010)
13. G. Schmid, *Nanoparticles: from Theory to Application* (Wiley, New York, 2004)
14. A. Bardhan, C.K. Ghosh, M.K. Mitra, G.C. Das, S. Mukherjee, K.K. Chattopadhyay, Solid State Sci. **12**, 839 (2010)
15. R.M. Mohamed, M.M. Rashad, F.A. Haraz, W. Sigmund, J. Magn. Magn. Mater. **322**, 2058 (2010)
16. K. Maaz, A. Mumtaz, S.K. Hasanain, A. Ceylan, J. Magn. Magn. Mater. **308**, 289 (2007)
17. X.M. Liu, S.Y. Fu, L.P. Zhu, J. Solid State Chem. **180**, 461 (2007)
18. Y. Cheng, Y. Zheng, Y. Wang, F. Bao, Y. Qin, J. Solid State Chem. **178**, 2394 (2005)
19. P. Lavela, J.L. Tirado, J. Power Sources **172**, 379 (2007)
20. M. George, A.M. John, S.S. Naira, P.A. Joy, M.R. Anantharaman, J. Magn. Magn. Mater. **302**, 190 (2006)
21. A. Baykal, N. Kasapoglu, Y. Koseoglu, M.S. Toprak, H. Bayrakdar, J. Alloys Compd. **464**, 514 (2008)
22. B. Baruwati, S.V. Manorama, Mater. Chem. Phys. **112**, 631 (2008)
23. S. Vivekanandhan, M. Venkateswarlu, N. Satyanarayana, Mater. Lett. **58**, 2717 (2004)
24. M. Salavati-Niasari, F. Davar, T. Mahmoudi, Polyhedron **28**, 1455 (2009)
25. N.S. Gajbhiye, S. Prasad, Thermochim. Acta **285**, 325 (1996)
26. R. Raeisi Shahraki, M. Ebrahimi, J. NanoStruct. **2**, 413 (2013)
27. M. Shakib Nahad, G. Mohammadi Ziarani, A. Badiei, A. Bananc, J. NanoStruct. **3**, 395 (2013)